Bifurcations of oscillatory and rotational solutions of double pendulum with parametric vertical excitation

Michal Marszal, Krzysztof Jankowski, Przemyslaw Perlikowski,
Tomasz Kapitaniak

Division of Dynamics, Lodz University of Technology

Abstract

This paper investigates dynamics of double pendulum subjected to vertical parametric kinematic excitation. It includes detailed bifurcation diagrams in two parameters space (excitation's frequency and amplitude) for both oscillations and rotations in the domain of periodic solutions.

Keywords : double pendulum, bifurcation analysis, basins of attraction, parametric excitation

1 Introduction

The construction of parametrically excited double pendulum is quite simple but its dynamics is very complex. There is still lack of complete bifurcation diagrams of oscillatory and rotational motions. The influence of the parametric forcing on the dynamical system was investigated by many researchers. The different directions of excitation for the double pendulum are investigated in authors' thesis [6], [10].

The chaotic motion is observed, as indicated in [8] or in [9]. The full bifurcation diagrams for horizontally, elliptically and vertically excited single pendulum are presented by Horton et al [5].

The detailed description of the parametrically excited double pendulum, with a special emphasis on 2:2 interaction mode can be found in [16]. This work was further expand [17], where authors show general explanation of the mode interaction. Here theory was proofed by practical experiment.

The dynamical behaviour of the double pendulum, in the vicinity of a number of compound critical points and the conditions of stability for the steady state solutions, in relation to the parameters of the systems, were explored by [21], resulting in closed form, achieved using bifurcation analysis for periodic and quasi-periodic solutions.

The approach towards numerical analysis of chaos in double pendulum is presented in [18]. It reveals regular behaviour of the pendula at the zero energy limit, which is transformed into quasi-regular and globally chaotic motion, along with the energy increase. The bifurcation diagrams are not ordinary, due to energy application as the parameter, instead of one of the parameters occurring in the equations of motion.

Furthermore, an orthogonal double pendulum with a pivot point subjected to the excitation is also described in [13]. The used method of averaging allows to investigate the resonant responses of the system, yielding to bifurcation analysis of the steady state constant solutions. It indicates the coexistence of planar and non-planar harmonic motion for relatively large base excitations. Taking into consideration certain regions of parameter space, those motions become unstable and may bifurcate to quasi-periodic motion with changing amplitude with slow and fast frequency. Mentioned quasi-periodic motion is prone to lose stability and lead to chaotic, amplitude-modulated

motion. Another approach towards investigation of the excited double pendulum is shown in [14]. It documents the parametric resonance causing the stable downward vertical equilibrium and the the stabilization of the unstable upward equilibrium state by subjecting the whole system to the high-frequency motion. The issue of excited pendulum was also elaborated by A. Belyakov in [1]. He presented planar rotational motion of the mathematical pendulum with an elliptical excitation analysis, basing on the exact solutions for the circular trajectory and no gravity. Derivation of existence and stability of these solutions, allows to find approximate solutions for high and low linear damping, providing not small excitation amplitudes.

In article [19], J.J. Thomsen examines the non-linear dynamics of the elastically restrained double pendulum with non-conservative follower-type loading and linear damping for the presence of chaotic motion. It was revealed, that static equilibrium solutions, stable periodic motion and initially large changes in amplitude due to a destabilizing effect of both linear and non-linear forces, are all the result of a small, local non-linear perturbation. A global numerical analysis proved, that theoretical assumptions concerning occurrence of the chaotic motion in these regions are correct. Moreover, the combination of bifurcation cascade of static equilibrium points together with non-linear destabilization may be treated as the cause of chaos trigger. The very similar system is presented in [15], however the investigation concerns destabilisation of the equilibrium position of the double pendulum with elastic end support and follower force loading. Since in Lyapunov criterion (for determining Lyapunov exponents from a time series, see [20]) is a critical case, non-linear analysis was performed, utilising centre manifold theory. The occurrence of heterochnic orbits suggested possibility of divergent and periodic flutter motion, however chaotic motion is also possible.

This paper is organized as follows: in section 2, the considered model of double pendulum is presented. Section 3 is devoted to the numerical study of the bifurcation diagrams, performed in two parameters space, namely excitation frequency and amplitude, as well as in one parameter space (i.e. amplitude) and basins of attractions. Finally, our results are summarised in section 4.

2 Investigated system

In this paper a system of double pendulum excited vertically is described. The system consists of planar double pendulum with non-elastic limbs. It is assumed that pendula are weightless with point masses m on each end respectively. The pivot point is vertically excited by parametric kinematic excitation. The excitation has amplitude A, excitation frequency is equal to ω, l denotes the length of each pendulum, c is a dumping coefficient on the pendula' nodes.

In order to derive the equations of motion (4) (5) second order Lagrange's equations are used. For the system presented in Figure 1, the kinetic energy T is formulated as shown:

$$T = \frac{1}{2}m(2A^2\omega^2\cos^2(\omega t) + l(2l(\frac{\mathrm{d}\theta_1}{\mathrm{d}t})^2 + \frac{\mathrm{d}\theta_2}{\mathrm{d}t}(-2A\omega\cos(\omega t)\sin\theta_2 + l\frac{\mathrm{d}\theta_2}{\mathrm{d}t}) + \frac{\mathrm{d}\theta_1}{\mathrm{d}t}(-4A\omega\cos(\omega t)\sin\theta_1 + 2l\cos(\theta_1-\theta_2)\frac{\mathrm{d}\theta_2}{\mathrm{d}t}))) \tag{1}$$

Whereas the potential energy V is given by (2):

$$V = -mlg(-3 + 2\cos\theta_1 + \cos\theta_2) \tag{2}$$

Finally, the Rayleigh's dissipation function D takes the form:

$$D = \frac{1}{2}c\left(\left(\frac{\mathrm{d}\theta_1}{\mathrm{d}t}\right)^2 + \left(\frac{\mathrm{d}\theta_1}{\mathrm{d}t} - \frac{\mathrm{d}\theta_2}{\mathrm{d}t}\right)^2\right) \tag{3}$$

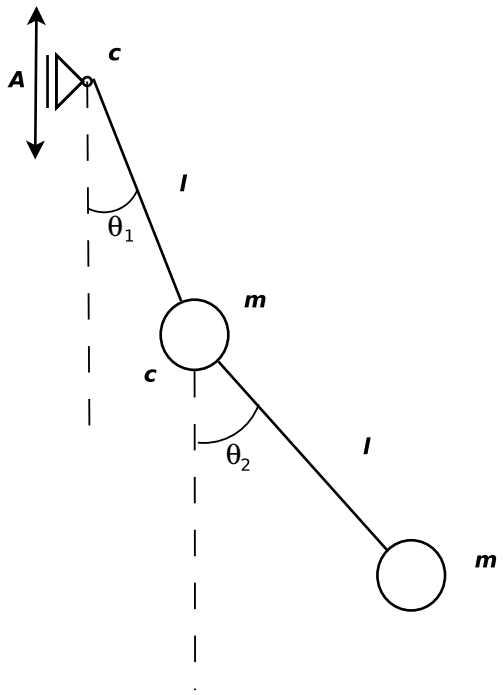

Figure 1: Scheme of the investigated system

Putting (1) (2) (3) into second order Lagrange equations and after some mathematical operations one obtains equations of motions (4) (5).

$$ml^2\left[2\frac{\mathrm{d}^2\theta_1}{\mathrm{d}t^2}+\frac{\mathrm{d}^2\theta_2}{\mathrm{d}t^2}\cos\left(\theta_1-\theta_2\right)\right]+2ml\sin\theta_1\left(g+A\omega^2\sin\omega t\right)+c\left(2\frac{\mathrm{d}\theta_1}{\mathrm{d}t}-\frac{\mathrm{d}\theta_2}{\mathrm{d}t}\right)$$
$$+ml^2\left(\frac{\mathrm{d}\theta_2}{\mathrm{d}t}\right)^2\sin\left(\theta_1-\theta_2\right)=0 \tag{4}$$

$$ml^2\left[\frac{\mathrm{d}^2\theta_1}{\mathrm{d}t^2}\cos\left(\theta_1-\theta_2\right)+\frac{\mathrm{d}^2\theta_2}{\mathrm{d}t^2}\right]+ml\sin\theta_2\left(g+A\omega^2\sin\omega t\right)+c\left(\frac{\mathrm{d}\theta_2}{\mathrm{d}t}-\frac{\mathrm{d}\theta_1}{\mathrm{d}t}\right)$$
$$-ml^2\left(\frac{\mathrm{d}\theta_1}{\mathrm{d}t}\right)^2\sin\left(\theta_1-\theta_2\right)=0 \tag{5}$$

In the next part of this paper dimensionless parameters are used: ${\omega_0}^2=\frac{g}{l}$, $\gamma=\frac{\omega}{\omega_0}$, $\rho=\frac{c}{\omega_0 ml^2}$, $\tau=\omega_0 t$, $\beta=\frac{A}{l}$, symbols $\ddot{}$ and $\dot{}$ denote $\frac{\mathrm{d}^2}{\mathrm{d}\tau^2}$ and $\frac{\mathrm{d}}{\mathrm{d}\tau}$ respectively. These parameters yield to dimensionless equations:

$$2\ddot{\theta_1} + \ddot{\theta_2}\cos(\theta_1 - \theta_2) + 2\sin\theta_1\left(1 + \beta\gamma^2\sin\gamma\tau\right) + \rho\left(2\dot{\theta_1} - \dot{\theta_2}\right) + \dot{\theta_2}^2\sin(\theta_1 - \theta_2) = 0 \quad (6)$$

$$\ddot{\theta_1}\cos(\theta_1 - \theta_2) + \ddot{\theta_2} + \sin\theta_2\left(1 + \beta\gamma^2\sin\gamma\tau\right) + \rho\left(\dot{\theta_2} - \dot{\theta_1}\right) - \dot{\theta_1}^2\sin(\theta_1 - \theta_2) = 0 \quad (7)$$

In the numerical calculations we use following value of dimensionless parameter $\rho = 0.04$.

In order to calculate the natural frequencies of the system, the equations (7) are linearised regardless of damping and excitation components.

$$\begin{aligned} 2\ddot{\theta_1} + \ddot{\theta_2} + 2\theta_1 &= 0 \\ \ddot{\theta_1} + \ddot{\theta_2} + \theta_2 &= 0 \end{aligned} \quad (8)$$

The natural frequencies calculated from the equations (8) are $\omega_1 = \sqrt{2 - \sqrt{2}}$, $\omega_2 = \sqrt{2 + \sqrt{2}}$, which is $\omega_1 = 0.765$, $\omega_2 = 1.848$.

3 Results

In this section results of the numerical analysis are presented, which include: the bifurcation diagrams in two parameters space (excitation frequency γ vs. amplitude of excitation β), bifurcation diagrams in one parameter space and basins of attractions. The tool for numerical analysis is Auto 07P [3] and authors' own programme using well-known 4th order Runge-Kutta method, with adaptive step size, from GNU GSL library version 1.15 [4]. The stability of periodic solutions is checked using Floquet multipliers [7]. In order to model physical behaviour of the system, the chosen range of parameters is as follows : $\gamma \in [0, 5]$, $\beta \in [0, 3]$.

The system poses three main characteristic regimes of motion. The first one is when the excitation (parametrised by frequency γ and amplitude β), which is in vertical direction, is not big enough to start pendula motion. In such a case pendula are in stable fixed point $\theta_1 = \theta_2 = 0$. The other fixed points : ($\theta_1 = 0$, $\theta_2 = \pi$), ($\theta_1 = \pi$, $\theta_2 = 0$), ($\theta_1 = \theta_2 = \pi$) are unstable.

Provided that sufficient energy is delivered to the system via excitation, it is possible to observe oscillatory motion. Pendula destabilize and after transient time both tends to synchronize with each other in phase (i.e. $\theta_1 = \theta_2$, $\dot{\theta}_1 = \dot{\theta}_2$), in such a way that one may treat upper and lower pendula as one pendulum. Results for oscillatory motion are described in details in chapter 3.1.

Finally, providing higher energy to the system (especially for high frequency γ) it is possible to obtain rotations. If this is the case, after transient time the pendula rotate together (i.e. $\theta_1 = \theta_2$), just as in the oscillatory motion, as one pendulum. From the point of view of possible application of double pendulum as electric power generator these types of solutions are particularly important for an engineer. Results for rotational motion are described in details in chapter 3.2.

The section is divided into three subsections: subsection 3.1 oscillatory solutions, subsection 3.2 rotations and subsection 3.3 basins of attractions. In subsection 3.1 a case where both pendula oscillate is presented, which is typical for smaller values of excitation frequency γ. In a case, where more energy is delivered to the system (i.e. for higher values of excitation frequency γ or excitation amplitude β), it is easier to set pendula in rotational motion, which is the topic of subsection 3.2 rotations. Finally, the influence of the initial conditions of the system on the results is illustrated by means of basins of attractions in subsection 3.3.

3.1 Oscillatory solutions

In the Figure 2(a) solutions for oscillatory motion of pendula are presented. The oscillatory periodic solutions are found usually for smaller energy delivered to the system (i. e. for smaller values of excitation frequency γ or excitation amplitude β). The system has enough energy to start its motion, however, not enough for the pendula to start rotation. In the investigated cases the pendula oscillate synchronised in phase (the lower pendulum follows the upper one). Numerical calculations find basically two locking ratios for oscillatory motion 1:1:1, 2:1:1 (i.e. excitation period : upper pendulum period : lower pendulum period) The Figure 2(a) focuses on 1:1:1 resonances and presents the borders of different solutions in two dimensional space (γ, β). The black solid curve represents the beginning of motion, when pendulum leaves the equilibrium state at stable fixed point (i.e. $\theta_1 = \theta_2 = \dot{\theta}_1 = \dot{\theta}_2 = 0$). It is worth mentioning, that tip of this curve corresponds to the value of natural frequency $\omega_1 = 0.765$ calculated in Chapter 2. The pendula oscillate synchronised in phase. Figure 2(b) shows the bifurcation scenario in one parameter space (β, $max(\theta_1)$). The value of excitation frequency is set to $\gamma = 0.68$. The pendula starts motion for $\beta = 1.60$, which corresponds to black curve from Figure 2(a). This can be mapped in the Figure 2(b) as an intersection with β-axis. The grey dashed line presents unstable orbits, while the solid black one stable orbits. Three stable regions are encountered, which start in saddle-node (SN) and end in period doubling (PD) bifurcations. Their equivalents in two parameters continuation can be found on the Figure 2(a), marked with respective colors (thick lines mark SN bifurcations and solid lines PD bifurcations).

The Figure 2(c) presents borders of oscillatory periodic solutions for $2:1:1$ resonance. Here, five curves are found showing different types of bifurcations. The purple one, represents the beginning of motion. Above this curve the stable fixed point ($\theta_1 = \dot{\theta_1} = \theta_2 = \dot{\theta_2} = 0$) becomes unstable and pendula start to oscillate. For values of excitation frequency lower then $\gamma = 1.535$ the born solutions are unstable (subcritical bifurcations), while for higher frequencies solutions are stable (supercritical bifurcations). The black line corresponds to saddle-node bifurcations, where the unstable solutions coming form the purple curve can change stability properties. The next curve (blue) represents the symmetry breaking bifurcations, hence the motion of pendula become asymmetrical with respect to the equilibrium position. As it is well known [11, 2] two mirror states are observed (one shifted in clockwise and second one in counter-clockwise direction). The last one, brown line, also indicates a state when pendula leave the equilibrium and start period-2 oscillations. The red curve presents the beginning of motion.

To have a good understanding what happened in the vicinity of resonance tongue ($\gamma = 1.535$) we compute three one parameter bifurcations diagrams, as shown in Figure 2(d). The parameters are $\gamma = 1.2$ (red line), $\gamma = 1.4$ (blue line) and $\gamma = 1.7$ (black line). Gray lines in Figure 2(d) correspond to positions of aforementioned one parameter diagrams. As previously, the solid lines indicate stable and dashed lines unstable solutions. The red line ($\gamma = 1.2$) for $\beta = 0.591$ begins in the subcritical bifurcation, so the solutions along this curve are unstable. Hence, for $\beta = 0.043$ we observe the saddle-node bifurcation, where curve turns but does not stabilize. Finally, for $\beta = 0.266$ the symmetry of this unstable solution is broken. The blue line ($\gamma = 1.4$) starts also in subcritcal bifurcation, hence solutions are unstable. For $\beta = 0.022$ we observe stabilization in the saddle-node bifurcation. Finally, for $\beta = 0.208$ the symmetry breaking bifurcations occur. The last curve for $\gamma = 1.7$ (black line) shows different scenario. The bifurcation where the motion originates from is supercritical, so from beginning the solutions are stable. The change of stability properties occurs for $\beta = 0.42$ in the symmetry breaking bifurcation. All above described scenarios are different and can be treated as reference bifurcation sequences. Each of them correspond to regions between cross-sections of two parameter bifurcation lines shown in Figure 2(c).

The curves obtained using the method of continuation are later compared with the results from numerical integration of the system equations of motions (6) (7). In Figure 3 the results are mapped with colored regions depending on the type of motion (oscilation, rotation), order of periodicity. Additionally, curves from earlier figures are added in order to show the comparison between these 2

method of system examining. The algorithm used in producing the color regions, creates series of bifurcation diagrams along with excitation frequency γ for different values of excitation amplitude β. It analyses the obtained results, the order of periodicity and character of motion (oscillations, rotations). In case of oscillations, it is obvious, that the black curve from Figure 2, representing the beginning of motion can be mapped by the green region of period-1 solution. The corresponding region for other curves presented in the Figure 2 (saddle-node, period doubling pairs) can be found in the Figure 3(b). It is especially clear, that solid lines for period doubling borders match region calculated by numerical integration (green to red transition). For the brown curve from Figure 2(c) describing the 2:1:1 resonances, it is possible to find its equivalent on the Figure 3(c). The red region indicating period-2 oscilation, correspond to the beginning of motion character of brown curve. The red curve from Figure 2(c) matches with period-2 region in the Figure 3(c). This is a very clear tongue of resonance 2:1:1.

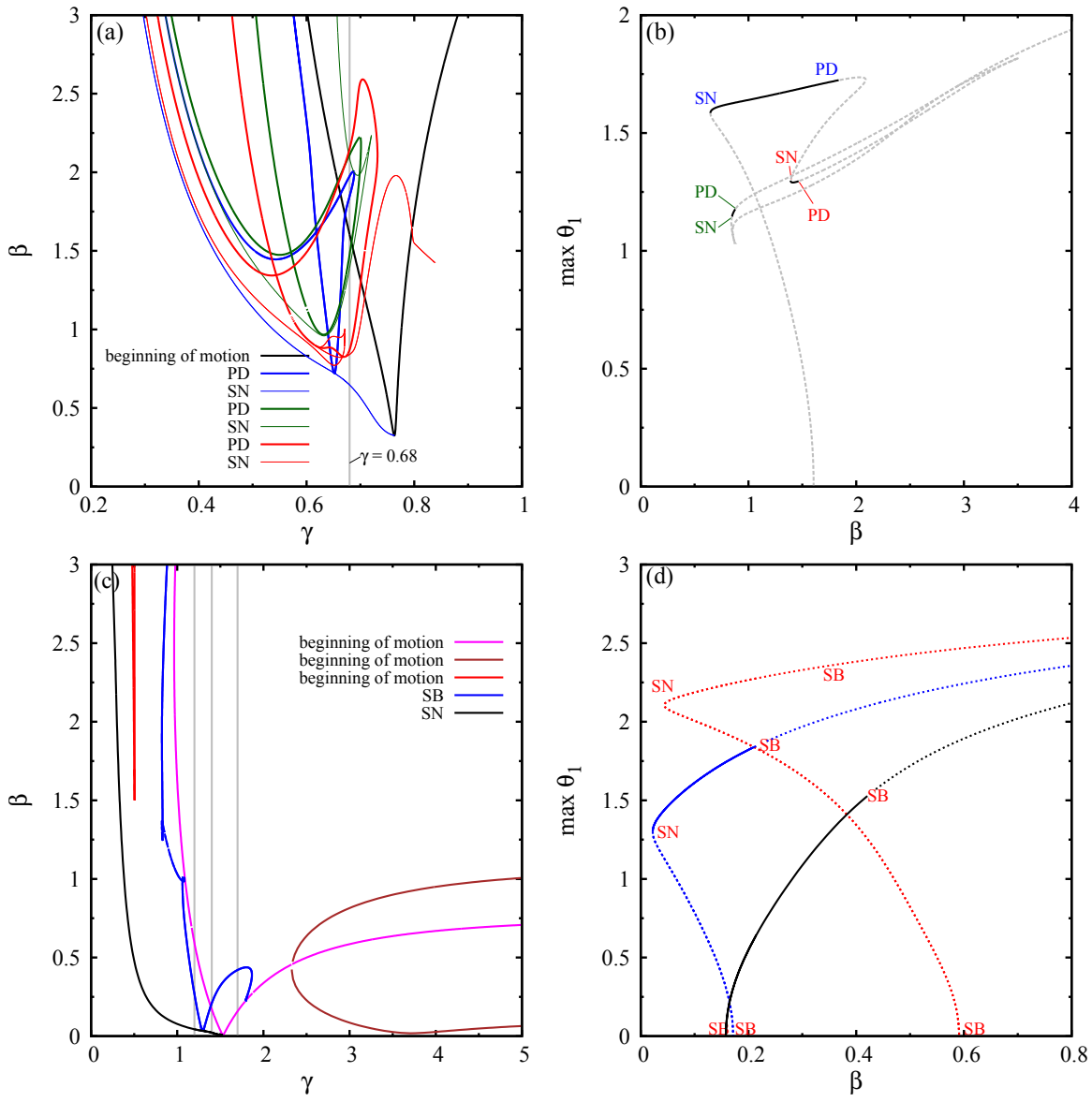

Figure 2: Bifurcation diagrams of oscillations the double pendulum (Figure 1) in two parameter space (γ,β). (a) Diagram representing 1:1:1 resonance. The thick lines apart from the black one represent saddle node bifurcation, while the thin lines represent period doubling. (b) One parameter space (β, $max\theta_1$) continuation for $\gamma = 0.68$, thick line represent stable solution, while dashed line unstable. (c) Diagram representing 2:1:1 resonance. (d) One parameter space continuation for: $\gamma = 1.2$ - red , $\gamma = 1.4$ - blue, $\gamma = 1.7$ - black. Abbreviations of bifurcations: SN - saddle-node, PD - period doubling and SB - symmetry breaking.

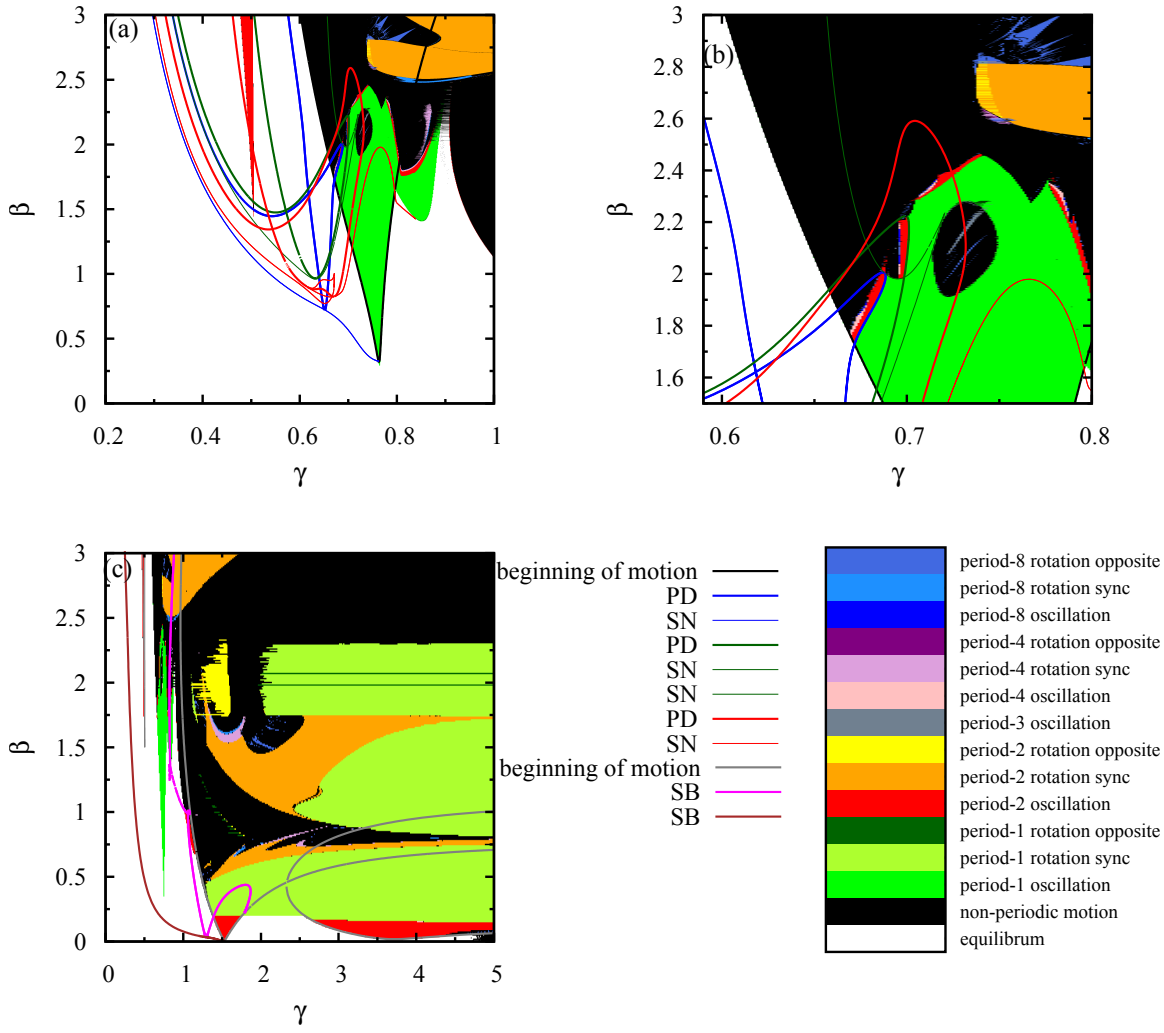

Figure 3: Bifurcation diagrams of oscillations of the double pendulum (Figure 1) in two parameter space (γ,β) using 2 methods. (a) Curves from Figure2(a) (1:1:1 resonance) . (b) Detailed view on Figure 3(b). (c) Curves from Figure2(c) (2:1:1 resonance). Initial conditions for numerical integration ($\theta_1 = \pi$, $\dot{\theta}_1 = -5$, $\theta_2 = \pi - 0.01$, $\dot{\theta}_2 = 5$). Abbreviations of bifurcations: SN - saddle-node, PD - period doubling and SB - symmetry breaking.

3.2 Rotations

Figure 4 presents bifurcation curves for rotating motion of the pendulum. The rotating motion happens for bigger values of excitation frequency γ. For most of the cases both pendula are rotating. There exists several cases for rotating pendula. The 2 major ones are both pendula rotating clockwise and both pendula rotating counter-clockwise. The direction of rotation depends mainly on the initial conditions applied to the system. However,in periodic domain there exist another combination when the rotation of pendulua are in the opposite direction. The boarders of obtained solutions in two parameters spaced obtained by AUTO software are presented in the Figure 4. The possible combinations (i.e. direction of oscillations) of rotations, computed using numerical integration are presented on Figure 5. Let us focus on the borders of periodic solutions, using continuation method (Figure 4) and how they match the results from numerical integration. The cyan curve in the Figure

4 represent 1:1:1 branching point. In that case, the results obtained using using continuation and numerical integration converge, particularly in the bottom region of the discussed curve. Significant number of period doublings (2:1:1 resonance) are found (3 cases). They are marked in the Figure 4 and Figure 5 as blue curves. The first one can be found in region $\gamma \in [2.5, 5]$ $\beta = 0.75$ matches the numerical representation from Figure 5. The detailed can be seen in the Figure 4(b). The next period doubling worth mentioning is located in the range $\gamma \in [2.5, 5]$ $\beta \in [1, 2.5]$. Once again the result from continuation method converge with the numerical integration. However, in this case only to some extent. The 3rd 2:1:1 period doubling located left from the previously discussed curve, has only partial coverage in numerical integration result.

Two toruses are to be found in the range $\gamma \in [2.5, 5]$ $\beta = 0.75$, red (2:1:1) and green(4:1:1). As well as in previous cases the numerical integration equivalent can be found for the above mentioned curves. Moving our attention to the left top corner of the Figure 4(a) (detailed view Figure 4(c)), one can observe saddle node bifurcation 2:1:1 resonance and small period doubling region 8:4:4. These findings are confirmed also by numerical integration (see Figure 5).

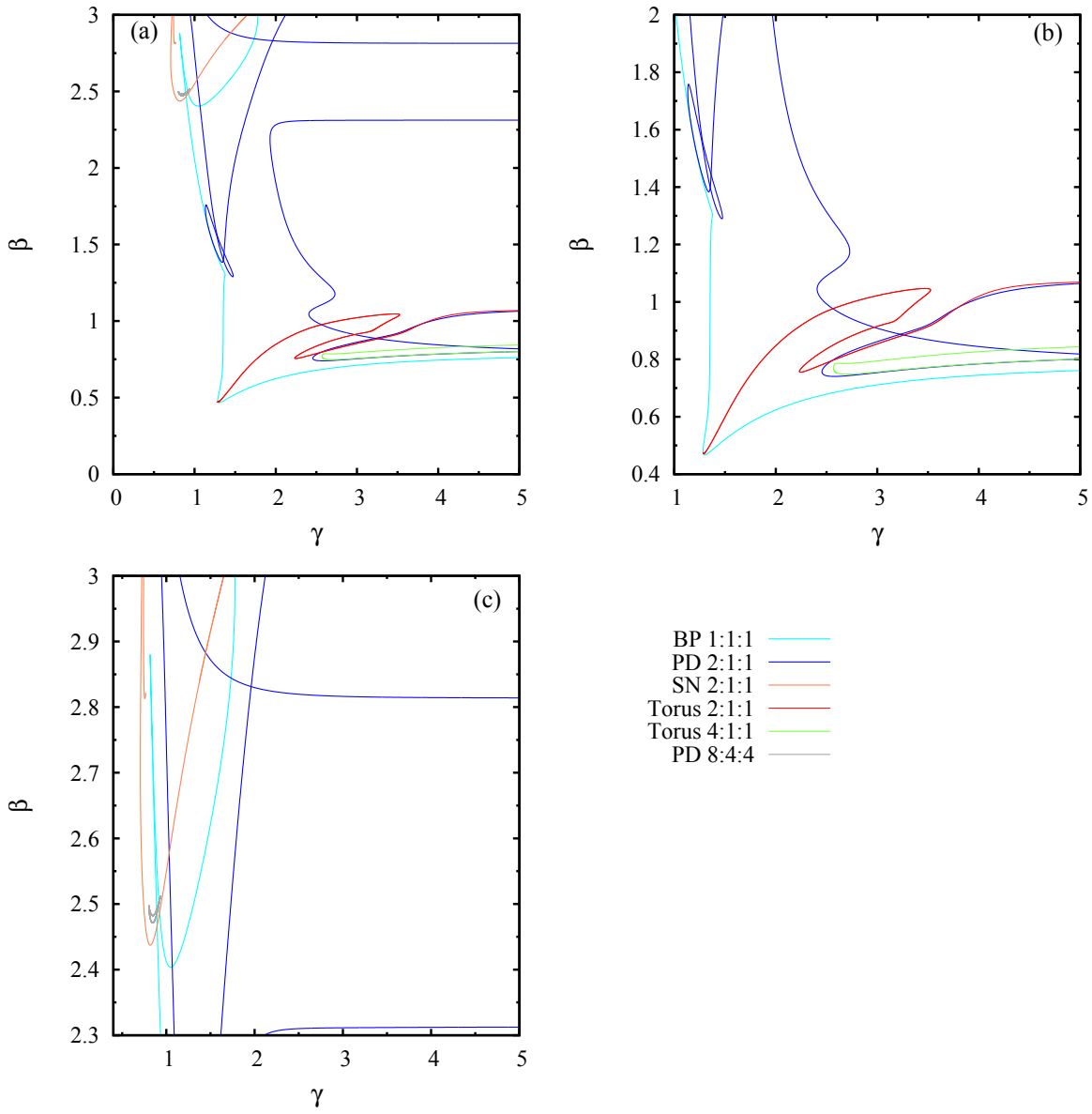

Figure 4: Bifurcation diagrams of rotations of the double pendulum (a) Two parameters bifurcation (excitation frequency γ vs. excitation amplitude β) for rotational solutions. (b), (c) Detailed view of (a). Abbreviations of bifurcations: SN - saddle-node, PD - period doubling, BP - branching point and SB - symmetry breaking.

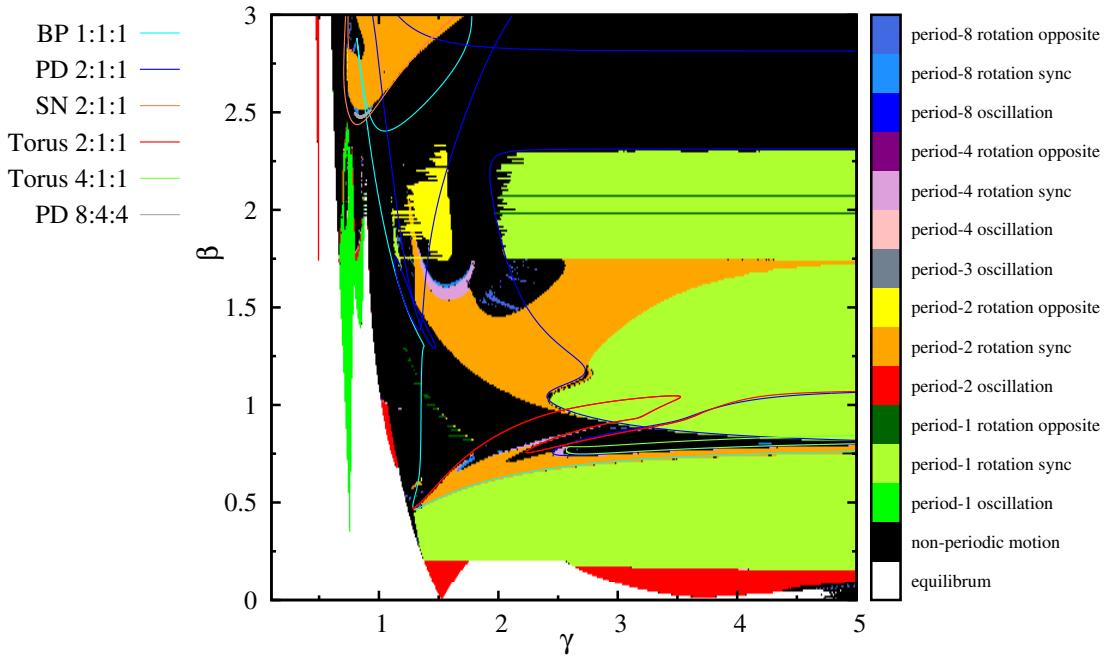

Figure 5: The rotation curves in two parameter space (γ, β). Each color of background represent different period order and type of motion (i.e. oscillation, rotations). Initial conditions for numerical integration ($\theta_1 = \pi$, $\dot{\theta}_1 = -5$, $\theta_2 = \pi - 0.01$, $\dot{\theta}_2 = 5$). Abbreviations of bifurcations: SN - saddle-node, PD - period doubling, BP - branching point and SB - symmetry breaking.

3.3 Basins of attraction

A phenomena of coexistence of solutions is very often encountered in non-linear dynamics. Therefore, in order to check if stable period solutions coexist, the system is checked using basins of attractions for different configuration of parameters. This section focuses basins of attraction. The software used for that purpose is Dynamics 2 [12]. The chosen values of parameters are: $\gamma = 0.68$, $\beta = 0.85$ and $\gamma = 0.75$, $\beta = 1.5$ which correspond to the regime of periodic oscillations. Because of the fact, that the investigated systems has four-dimensional phase space, the obtained results are two-dimensional cross-sections of four dimensional phase space.

Figure 6(a) is in (θ_1, θ_2) space, where $\gamma = 0.68$ $\beta = 0.85$, $\dot{\theta}_1 = 0.5$, $\dot{\theta}_2 = 0.5$ and $\theta_1 \in [-\pi, \pi]$ and $\theta_2 \in [-\pi, \pi]$. One can observe 2 symmetric basins (marked as white and red respectively). The blue area attracts to the stable solution (i.e. $\theta_1 = 0$, $\dot{\theta}_1 = 0$, $\theta_2 = 0$, $\dot{\theta}_2 = 0$). The white and red basins attracts the solution to periodic solution of period-1. In case of Figure 6(b) the cross section through parameter space is done for different space variables. The basin is in (θ_2, $\dot{\theta}_2$) space (position and velocity of the second pendulum), $\gamma = 0.68$ $\beta = 0.85$, $\theta_1 = -\frac{\pi}{2}$, $\dot{\theta}_1 = 2$ and $\theta_2 \in [-\pi, \pi]$, $\dot{\theta}_2 \in [-5, 5]$. Here, once again one deals with symmetric basins. 3 regions are found: the cyan attracts to equilibrium (green dot), the purple basin attract to period-1 oscillations, while white basin also attracts to period-1 oscillation. One can notice a central symmetry with ($\theta_2 = 0$, $\dot{\theta}_2 = 0$) as reflection point. Finally, the last basin presented in the Figure 6(c) indicates 2 basins of attraction. The phase space is cut along (θ_2, $\dot{\theta}_2$) plane, for $\theta_1 = -\frac{\pi}{2}$, $\dot{\theta}_1 = 2$, $\gamma = 0.75$, $\beta = 1.5$. The detected basins of attractions attract to period-1 oscillation, which are central symmetrical with reflection point $(0, 0)$. The green dot attracts to white basin, while the blue one to the purple basin.

Looking at the every obtained basing one may draw a conclusion that the solution depends

strongly on the initial conditions. While the basins for the investigated systems are mostly symmetrical and attracts to the same type of pendula motion, there is a significant large basin that attracts to stable fixed point at pendula equilibrium.

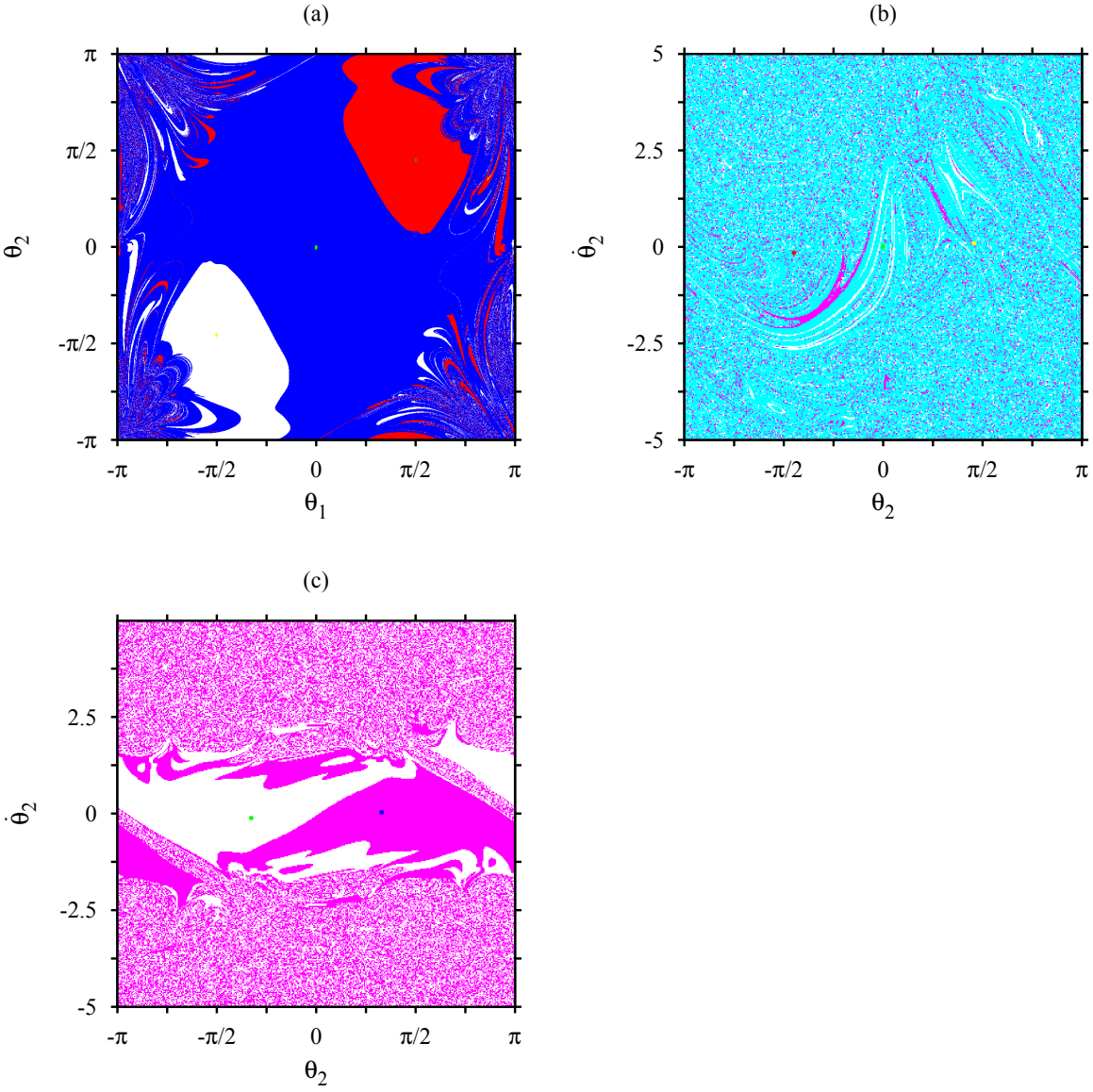

Figure 6: Basin of attractions in different planes and parameters: (a) plane (θ_1, θ_2), $\gamma = 0.68$, $\beta = 0.85$, $\dot{\theta}_1 = 0.5$, $\dot{\theta}_2 = 0.5$ (b) plane $(\theta_2, \dot{\theta}_2)$,$\gamma = 0.68$, $\beta = 0.85$, $\theta_1 = -\frac{\pi}{2}$, $\dot{\theta}_1 = 2$ (c) plane $(\theta_2, \dot{\theta}_2)$, $\gamma = 0.75$, $\beta = 1.5$, $\theta_1 = -\frac{\pi}{2}$, $\dot{\theta}_1 = 2$

4 Conclusions

This paper presents broad numerical analysis of the dynamics of double pendulum excited vertically. Bifurcation diagrams in two parameter space (excitation frequency γ vs. excitation amplitude β), as a continuation of periodic solutions, are shown. For oscillations of the pendula two locking ratios

are observed (i.e 1:1:1 and 2:1:1). However, in case of rotational solutions one obtains also different locking ratios, such as 4:1:1 or 8:4:4. The emerging of resonance zone happens about excitation frequency $\gamma = 0.7$. Additionally, an iterative numerical integration, in order to check the results from continuation, is performed. The result of this comparison is successful, because it is possible to observe similar regions using both methods. Finally, the basins of attractions give the answer on influence of the initial conditions on the solutions. Symmetrical basins are obtained for most of the cases with 2 periodic basins.

Acknowledgements

This work has been supported by the Foundation for Polish Science, Team Programme under project TEAM/2010/5/5.
The authors declare that there is no conflict of interests regarding the publication of this article.

References

[1] A.O. Belyakov. On rotational solutions for elliptically excited pendulum. *Physics Letters A* 375, 2011.

[2] P. Brzeski, P. Perlikowski, S. Yanchuk and T. Kapitaniak. The dynamics of the pendulum suspended on the forced Duffing oscillator. *Journal of Sound and Vibration* 331, 2012.

[3] E.J. Doedel and B.E. Oldeman. *Auto-07P: Continuation and bifurcation software for ordinary differential equations*. Concordia University, Montreal, 2009.

[4] M. Galassi, J. Davies, J. Theiler, B. Gough, G. Jungman, P. Alken, M. Booth, and F. Rossi. *GNU Scientific Library, Reference Manual, Edition 1.15, for GSL Version 1.15*, 2011.

[5] B. Horton, J. Sieber, J.M.T. Thomson, and M. Wiercigroch. Dynamics of the Nearly Parametric Pendulum. *International Journal of Nonlinear Mechanics* 46, 2010.

[6] K. Jankowski. Dynamics of double pendulum with parametric vertical excitation. Master's thesis, Lodz University of Technology, 2011.

[7] I.U.A. Kuznetsov. *Elements of Applied Bifurcation Theory*. Number t. 112 in Applied Mathematical Sciences. Springer, 2004.

[8] R.W. Leven and B.P. Koch. Chaotic behaviour of a parametrically excited damped pendulum. *Physics Letters A* 86, 1981.

[9] R.W. Leven, B. Pompe, C. Wilke, and B.P. Koch. Experiments on periodic and chaotic motions of a parametrically forced pendulum. *Physica D: Nonlinear Phenomena* 16, 1985.

[10] M. Marszal. Dynamics of double pendulum with parametric horizontal excitation. Master's thesis, Lodz University of Technology, 2011.

[11] J. Miles. Resonance and symmetry breaking for the pendulum. *Physica D: Nonlinear Phenomena* 31, 1988.

[12] H.E. Nusse, J.A. Yorke, B.R. Hunt, and E.J. Kostelich. *Dynamics: Numerical Explorations*. Number t. 101 in Applied mathematical sciences. Springer, 1998.

[13] S. Samaranayake and A.K. Bajaj. Bifurcations in the dynamics of an orthogonal double pendulum. *Nonlinear Dynamics* 4, 1993.

[14] J.C. Sartorelli and W. Lacarbonara. Parametric resonances in a base-excited double pendulum. *Nonlinear dynamics* 69, 2012.

[15] R. Scheidl, H. Troger, and K. Zeman. Coupled flutter and divergence bifurcation of a double pendulum. *International Journal of Nonlinear Mechanics* 19, 1983.

[16] A.C Skeldon. Dynamics of a parametrically excited double pendulum. *Physica D: Nonlinear Phenomena* 75, 1994.

[17] A.C Skeldon and T. Mullin. Mode interaction in a double pendulum. *Physics Letters A* 166, 1992.

[18] T. Stachowiak and T. Okada. A numerical analysis of chaos in the double pendulum. *Chaos, Solitons and Fractals* 29, 2006.

[19] J.J. Thomsen. Chaotic dynamics of the partially follower-loader elastic double pendulum. *Journal of Sound and Vibration* 188, 1995.

[20] A. Wolf, J.B. Swift, H.L. Swinney, and J.A Vastano. Determining Lyapunov exponents from a time series. *Physica D: Nonlinear Phenomena* 16, 1985.

[21] P. Yu and Q. Bi. Analysis of non-linear dynamics and bifuractions of a double pendulum. *Journal of Sound and Vibration* 217, 1998.